

Localized polarons and conductive charge carriers: understanding $\text{CaCu}_3\text{Ti}_4\text{O}_{12}$ over a broad temperature range

Laijun Liu,[†] Shaokai Ren,[†] Jia Liu,[‡] Feifei Han,[†] Jie Zhang,[¶] Biaolin Peng,[§] Dawei Wang,^{*,||} Alexei A. Bokov,[⊥] and Zuo-Guang Ye[⊥]

[†]*Current address: College of Materials Science and Engineering, Guilin University of Technology, Guilin, 541004, China*

[‡]*Current address: State Key Laboratory for Mechanical Behavior of Materials, School of Materials Science and Engineering, Xi'an Jiaotong University, Xi'an 710049 China*

[¶]*Current address: Electronic Materials Research Laboratory-Key Laboratory of the Ministry of Education and International Center for Dielectric Research, Xi'an Jiaotong University, Xi'an 710049, China*

[§]*Current address: School of Physical Science & Technology and Guangxi Key Laboratory for Relativistic Astrophysics, Guangxi University, Nanning 530004, China*

^{||}*Current address: School of Microelectronics & State Key Laboratory for Mechanical Behavior of Materials, Xi'an Jiaotong University, Xi'an 710049, China*

[⊥]*Current address: Department of Chemistry and 4D LABS, Simon Fraser University, Burnaby, British Columbia, V5A 1A6, Canada*

E-mail: dawei.wang@mail.xjtu.edu.cn

Abstract

$\text{CaCu}_3\text{Ti}_4\text{O}_{12}$ (CCTO) has a large dielectric permittivity that is independent of the

probing frequency near the room temperature, which complicated due to the existence of several dynamic processes. Here, we consider the combined effects of localized charge carriers (polarons) and thermally activated charge carriers using a recently proposed statistical model to fit and understand the permittivity of CCTO measured at different frequencies over the whole temperature range accessible by our experiments. We found that the small permittivity at the lowest temperature is related to polaron frozen, while at higher temperatures the rapid increase is associated with the thermal excitation of polarons inducing the Maxwell-Wagner effect, and the final increase of the permittivity is attributed to the thermally activated conductivity. Such analysis enables us to separate the contributions from localized polarons and conductive charge carriers and quantify their activation energies.

Keywords

CCTO, dielectric response

1 Introduction

Materials with high dielectric permittivity have attracted much attention due to their numerous technological applications. $\text{CaCu}_3\text{Ti}_4\text{O}_{12}$ (CCTO) has a cubic perovskite structure and a giant relative permittivity of $10^4 \sim 10^6$ near the room temperature. While the dielectric permittivity of CCTO exhibits a very small temperature dependence between 100 K and 600 K, it drops rapidly to a value of ~ 100 below 100 K.¹⁻¹⁰ This overall behavior of CCTO is very different from either relaxors or normal ferroelectrics. It is established that the origin of such high permittivity is an extrinsic effect, which in polycrystalline CCTO is modeled with internal barrier layer capacitor (IBLC), consisting of semiconducting grains separated by thin insulating grain boundaries leading to high dielectric permittivity. Furthermore, the interface effect from electrodes or domain walls is suggested to also contribute to the high

permittivity especially in single crystals.

In addition, such remarkable dielectric properties also strongly depend on the probing frequency, which approximately follows the Arrhenius behavior. Similar phenomenon was also found in many manganites, cuprates, and nickelates, such as $\text{La}_{1-x}\text{Ca}_x\text{MnO}_3$,¹¹ $\text{Pr}_{0.7}\text{Ca}_{0.3}\text{MnO}_3$,¹² Tb/EuMnO_3 ,^{13–16} CuTa_2O_6 ,¹⁷ LaCuLiO_4 ,¹⁸ LaSrNiO_4 ,¹⁹ Li/Ti -doped NiO ,^{20,21} and $\text{Ba}(\text{Fe}_{0.5}\text{Nb}_{0.5})\text{O}_3$.^{22–26} Therefore, a better understanding of CCTO will also help to explain the dielectric properties of a large group of materials. For these materials, their low-temperature dielectric relaxation has been attributed to hopping of polarons, which are localized charge carriers interacting with phonons²⁷, between lattice sites with a characteristic timescale. The step-function-like decrease suggests a freezing temperature in the relaxation behavior following a glass-like process.

However, important questions regarding this type of materials remain unanswered. For instance, while it is known that the polaronic relaxation usually involves either a variable range hopping (VRH) or a nearest-neighbor hopping conduction process,^{28,29} an estimation of the activation energy, which is a key parameter for such process, is still missing. Moreover, at higher temperatures, the permittivity of such materials also include the contribution from thermally activated conducting electrons. The non-localized conductivity is not a pure *dc* conductivity, that is, high dielectric loss is accompanied by the increase of dielectric permittivity at low frequencies. It is unclear how important such contribution is to the total permittivity, which contains the effects of both thermally activated polarons and conductive charge carriers. As a matter of fact, for the permittivity of such materials, a complete description of their temperature dependence is unavailable over the temperature range accessible to experiments. It is worth noting that the Maxwell-Wagner model alone is not enough to understand the permittivity over the whole temperature range (see Eq. (5) below). Moreover, while the system may be modeled with a parallel RC equivalent circuit and results in the Arrhenius equation,³⁰ the physics underlying such phenomenon needs further understanding to establish connections between the RC circuits and charge carriers in the

system.

In this paper, we will answer the aforementioned questions using a statistical approach, which is based on macroscopic and phenomenological considerations of both thermally activated polarons and conductive charge carriers in CCTO. With this approach, we are able to propose an explicit formula to fit the permittivity over the whole temperature range accessible by experiments, which in turn enables us to separate the contributions from polaron and conductive charge carriers. Such separation finally allows us to estimate the activation energies of polarons, as well as conductive charge carriers. Since the analysis separates these two effects and offer some details regarding them, it will enhance our understanding of CCTO and similar materials, and provide useful clues to design or improve this type of materials.

2 Experimental Section

$\text{CaCu}_3\text{Ti}_4\text{O}_{12}$ (CCTO) powder was prepared by a molten salt method.³¹ The obtained CCTO powder was pressed into pellets of 15mm in diameter and ~ 1 mm in thickness. The pellets were sintered at 1060 °C in the air for 30 h. X-ray diffraction shows that the powder is of pure cubic perovskite phase. Both sides of the samples were first polished and then brushed with silver conductive paste, which is followed by a heat treatment at 550 °C for 30 min. Dielectric measurements were performed with an applied voltage of 500 mV using an Agilent 4294A impedance analyzer over the frequency range of 100 Hz to 1 MHz and over the temperature range from 90 K to 500 K.

3 Results and discussion

The temperature dependence of the loss factor of the CCTO sample is shown in Fig. 1. Below 300 K, the loss peaks shift to high temperature with the probing frequency, which shows a Debye-like relaxation. At high temperatures, the loss factor increases rapidly with temperature, suggesting a thermally activated process.

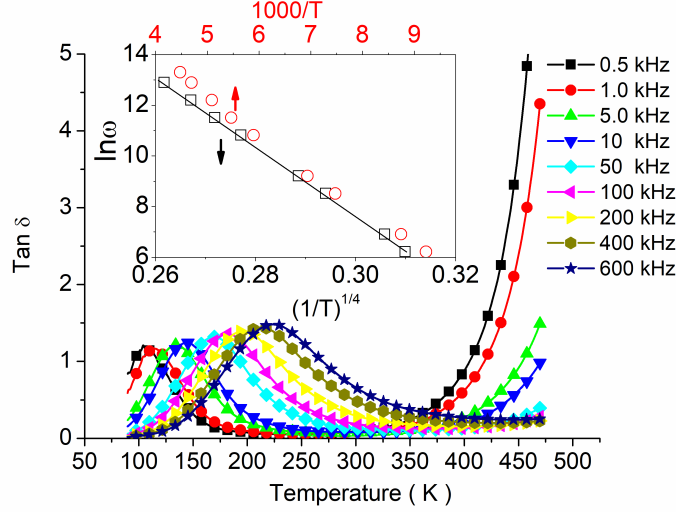


Figure 1: Temperature dependence of $\tan\delta$ of the permittivity of CCTO at various frequencies. Inset: temperature-dependent relaxation frequency ω scaled for thermally activated nearest-neighbor hopping of charges (open circles, top and left axes) and VRH (open squares, bottom and left axes). The solid line is the fitting curve of the experimental data (open squares) according to Eq. 1.

3.1 Dielectric relaxation

To understand the relaxation at low temperatures, we first analyze the behavior of the dielectric dissipation. The inset in Fig. 1 shows the temperature dependence of the relaxation frequency of CCTO, $\ln\omega$ vs $1/T^{1/4}$ (open squares), where ω is the position of the loss peak in the $\tan\delta$ versus $\ln\omega$ plots. We can clearly see that there is a very good linear relation between $\ln\omega$ and $1/T^{1/4}$.

On the other hand, if we plot $\ln\omega$ as a function of $1000/T$ (open circles), the result shows an approximate Arrhenius relation. According to this relation, the relaxation frequency at the infinite temperature and the activation energy are found to be 3.59×10^8 Hz and 130 meV, respectively. These values are in good agreement with that of perovskite materials,³² associated with the localization process of charge carriers. However, it is notable that a distinct deviation from the Arrhenius relation exists above ~ 200 K. Such a deviation has been found in polaron related relaxations of certain materials, such as CCTO^{27,28,33} and $\text{Sr}_{0.998}\text{Ca}_{0.002}\text{TiO}_3$.³⁴ The reason for the deviation from the Arrhenius law is likely the tran-

sition from a grain boundary-limited to bulk-limited conduction, consistent with the widely held "barrier layer model".^{35,36}

Therefore, according to our results and calculations, Mott's variable-range-hopping (VRH) model,³⁷ i.e.,

$$f = f_1 \exp \left[- (T_1/T)^{1/4} \right] \quad (1)$$

can be used to better fit the relaxation frequency, where f_1 and T_1 are two constants. The solid line in the inset of Fig. 1 is the fitting result of our experimental results according to Eq. 1. The values of f_1 and T_1 are determined to be 1.68×10^{21} Hz and 3.56×10^8 K, respectively. The value of T_1 of CCTO is similar to those of Li-doped La_2CuO_4 ³⁸ and Cu-doped BaTiO_3 ³⁹ while f_1 is much higher. According to the IBLC model, the relaxation frequency is related to dc conductivity and grain-boundary capacitance of CCTO²⁸. As a matter of fact, it was shown in Ref.²⁸ that f_1 has an approximate linear relation with the dc conductivity of the material. Therefore, f_1 does not represent the hopping frequency of polarons.

Since the VRH mechanism describes the low-temperature dielectric relaxation of CCTO ceramics well, it supports the idea that three-dimensional disorder effects dominate the relaxation behavior of CCTO's semiconducting phases. At this phase, the kinetic energy (due to the thermal excitation) is insufficient to excite charge carrier across the Coulomb gap, therefore Eq. 1 is mostly due to the hopping of charge carriers within small regions. Figure 1 thus provides strong evidence for the existence of (hopping) polarons in CCTO.

3.2 Permittivity

The temperature dependence of CCTO's permittivity measured at different frequencies is shown in Fig. 2. The rapid increase in the low-temperature region is intimately related to the polaron hopping. The curves in Fig. 2 have four stages: (i) a plateau region at the lowest temperatures (the exact temperature depends on the probing frequency; at 1 kHz, $T <$

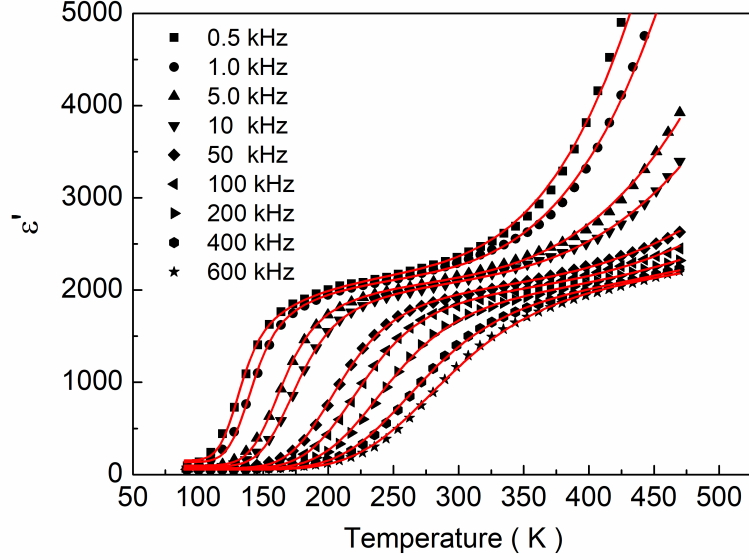


Figure 2: Temperature dependence of the real dielectric permittivity of the CCTO with different frequencies. The solid lines are the fitting results according to the Eq (4).

90 K), where polarons are frozen and the permittivity is below 100. (ii) As the temperature increases, the dielectric permittivity has a rapid rise (at 1 kHz, $90 < T < 150$ K), which is related to the thermal excitation of polarons inside grains. The polaron hopping leads to semiconducting grains, where charge carriers are able to move freely (but not beyond the grain boundaries). Consequently, such grains separated by thin insulating grain boundaries result in the Maxwell-Wagner effect, which significantly enhances the dielectric permittivity. (iii) A plateau region exists at even higher temperatures (at 1 kHz, $150 < T < 350$ K). (iv) Another rapid increase of dielectric permittivity at the highest temperatures, which can be attributed to the thermally activated conductivity over the bulk.

Looking carefully at these results, we can see some similarity to the temperature dependent permittivity of relaxors,⁴⁰ where it was found that contributions from different origins have varying weight over the whole temperature range. Interestingly, we find that the statistical approach adopted in Ref.⁴⁰ can also be used to understand the dielectric response of polarons in CCTO as well.

3.3 Fitting model

The Maxwell-Wagner relaxation model can be simplified as two alternating slabs having different dielectric permittivity (ε_g and ε_{gb} for grains and grain boundaries, respectively), conductivity (σ_g and σ_{gb} for grains and grain boundaries, respectively) and widths (l and d corresponding to grains and grain boundaries, respectively and $L = l + d$), one can approximately obtain the effective permittivity as^{41,42}

$$\begin{aligned}\varepsilon^* &= \frac{L}{l/(\varepsilon_g - i\sigma_g/\omega) + d/(\varepsilon_{gb} - i\sigma_{gb}/\omega)} \\ &= \varepsilon_\infty + \frac{\varepsilon_0 - \varepsilon_\infty}{1 + i\omega\tau} - i\frac{\sigma(\omega)}{\omega},\end{aligned}\tag{2}$$

where $\varepsilon_\infty = L/(l/\varepsilon_g + d/\varepsilon_{gb})$, $\varepsilon_0 = L(\sigma_{gb}\varepsilon_g + \sigma_g\varepsilon_{gb})/(l\sigma_{gb} + d\sigma_g)$, $\tau = (l\varepsilon_{gb} + d\varepsilon_g)/(l\sigma_{gb} + d\sigma_g)$, and $\sigma(\omega) = \sigma_g\sigma_{gb}/[(l\sigma_{gb} + d\sigma_g)(1 + i\omega\tau)]$. The dielectric permittivity shown in Eq. (2) consists of three contributions. The first is a constant determined by the permittivity of both the grain and its boundary. The second contribution is of Debye type with the relaxation time determined by the conductivity and permittivities. The third term describes the contribution from the conductivity of grains and grain boundaries. We can see that the relaxation time τ can strongly depend on the temperature if the conductivity of the system can change significantly with temperature.

The phenomenological model we propose is based on the Debye relaxation of polarons and the *ac* conductivity of conductive charge carriers. In this model, individual polarons are categorized into two groups. Our assumption is that the polarons need to be thermally excited to overcome a local energy minimum before they can have large contributions to the grain conductivity σ_g and permittivity ε_g . When the temperature is sufficiently low, most of the polarons charge can only move around its equilibrium position, their contribution to grain conductivity and permittivity is small and can be taken as an insulator, where the permittivity can be taken as a constant. As the temperature increases, more and more of

them can move on a larger spacial scale (but still bound by grain boundaries), jumping from one energy minimum to others, with their contribution to the conductivity and permittivity becoming much larger.

Similar to our statistical model for relaxors,⁴⁰ here we employ the Maxwell-Boltzmann distribution to estimate the number of active polarons relative to the inactive ones, where we need to introduce a potential well of average depth, E_b , to account for the constraint on the polarons. One important reason we can apply the model developed for relaxor is because polarons may be taken as individual particles as the dipoles in relaxors. Practically, the number of polarons with a kinetic energy exceeding the potential well $[N_1(E_b, T)]$ is given by

$$N_1(E_b, T) = N \sqrt{\frac{4}{\pi}} \sqrt{\frac{E_b}{k_B T}} \exp\left(-\frac{E_b}{k_B T}\right) + N \operatorname{erfc}\sqrt{\frac{E_b}{k_B T}}, \quad (3)$$

where N is the total number of polarons in the system, k_B is the Boltzmann constant, T is the temperature (in Kelvin), and erfc is the complementary error function. The total dielectric permittivity is then given by

$$\varepsilon(T, \omega) = \varepsilon_1(T, \omega) P_1(E_b, T) + \varepsilon_2(T, \omega) P_2(E_b, T), \quad (4)$$

where $\varepsilon_1(T, \omega)$ and $\varepsilon_2(T, \omega)$ describe the dielectric responses from the aforementioned two polaron groups, ω is the probing frequency, and $P_1(E_b, T) = N_1(E_b, T)/N$, $P_2(E_b, T) = 1 - P_1(E_b, T)$ account for the proportion of polarons in each group. We note that, according to Eq. (2), the permittivity in Eq. 4 result from not only the intrinsic polarization of polarons, but also the grain conductivity associated with the distribution of the thermally activated polarons, which is often described by the Maxwell-Wagner effect.

It has been found that the temperature where the dielectric permittivity is almost a step function strongly depends on the probing frequency, which approximately follows an Arrhenius behavior, therefore the Debye relaxation, i.e., $\varepsilon \sim 1/(1 + \omega^2 \tau_0^2)$ ⁴⁴ was chosen, where τ_0

is the temperature-dependent relaxation time. For a thermally activated process, it follows the Arrhenius law. Consequently, the permittivity will be $\varepsilon \sim 1/[1 + A^2\omega^2\exp(2E_a/T)]$, which is discussed by Jonscher⁴⁵ and follows the approach shown in Ref.⁴⁰.

In addition to the above analysis, we also need to consider the high-temperature dielectric response induced by the conductivity due to the thermally activated non-localized conductive charge carriers⁴³, which is accounted for by a new term (the last term in the equation below)

$$\varepsilon(T) = \frac{\varepsilon_1}{1 + \omega^2\tau_0^2\exp(-\theta/T)}P_1(E_b, T) + \varepsilon_2P_2(E_b, T) + \frac{\sigma\exp(-E_{\text{con}}/k_BT)}{\varepsilon_0\omega}, \quad (5)$$

where ε_1 , ε_2 , τ_0 and θ are constants at a given frequency ω , ε_0 is the vacuum permittivity, σ is the thermal activated conductivity, and E_{con} is the conductivity activation energy for conductive charge carriers' migration and transport.

The above Eq. (4) has clear physical meanings: (i) The first and second terms are the same as in Ref.⁴⁰ except that the analysis applies to polarons; (ii) The third term or the RHS is the contribution of conductive charge carriers, which is often associated with a thermal activation process.

3.4 Analysis using the fitting model

Having shown the explicit formula to describe the dielectric permittivity versus temperature, we now use Eq. (4) to fit $\varepsilon(T)$ of CCTO at different frequencies and show the results in Fig. 2 (solid line). The fitting curves are in very good agreement with experimental results. For CCTO, the E_b of the polarons exhibits very little dependence on the probing frequency. Therefore, we find $E_b = 0.19$ eV with a simple averaging procedure and use this value for all the fittings at different frequencies.

The activation energy for the conducting charge carriers E_{con} usually is more related to the composition rather than the probing frequency. From our fitting results, $E_{\text{con}}=0.25$ eV is also obtained with a simple averaging procedure. The θ value is 2100 K, which only

slightly changes with the probing frequency, while $\ln\tau_0$ is inversely proportional to the probing frequency ω . The good fitting in Fig. 2 shows the importance of polaronic conduction in the grains, whose relaxation was likely induced by the charge accumulation at the grain boundaries (because grain boundaries are less conductive), which reveals some connections between polarons and the IBCL model. We also note that the fitting parameters (e.g., E_{con}) depend on samples, especially their grain sizes and composition as discussed in Ref.⁴⁶.

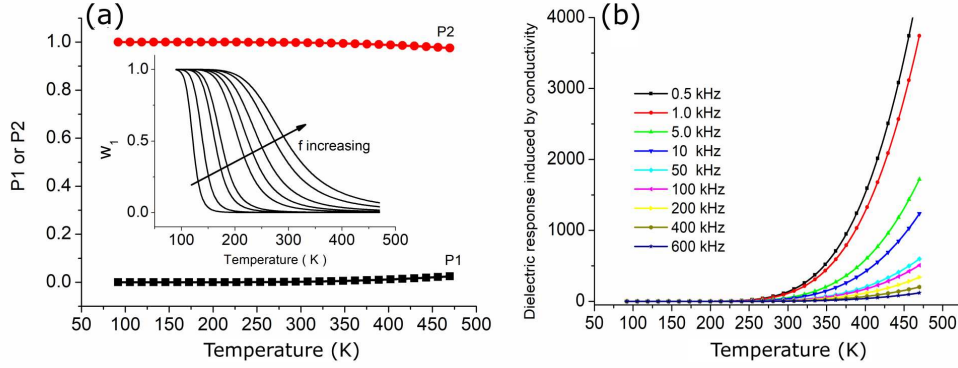


Figure 3: (a) The Maxwell-Boltzmann distribution (P_1 and P_2) and the $\varepsilon_1/[1 + \omega^2\tau_0^2\exp(-\theta/T)]$ (inset) vs temperature of the CCTO. (b) Temperature dependence on the dielectric response induced by conductivity.

To understand the dielectric response of CCTO, we also show $P_1(E_b, T)$, $P_2(E_b, T)$ and the function $\varepsilon_1/[1 + \omega^2\tau_0^2\exp(-\theta/T)]$ in Fig. 3(a). Clearly, $P_1(E_b, T)$ and $P_2(E_b, T)$ show little change as temperature increases, which is different from typical ferroelectric relaxors, such as $\text{Ba}(\text{Ti}_{1-x}\text{Zr}_x)\text{O}_3$ for $x > 0.3$ with smaller E_b .⁴⁶ This feature indicates that the number of “active” polarons which can overcome the potential confinement remain small (P_1 is small) over the experimental temperature range. However, the large value of ε_1 (1.25×10^6 to 8.97×10^9 depending on the probing frequency, which is also much larger than that of typical relaxors) indicates that those polarons are highly correlated and can make an important contribution to the total permittivity once they overcome E_b . The function $\varepsilon_1/[1 + \omega^2\tau_0^2\exp(-\theta/T)]$ describes the ability of polarons (which can overcome the potential well) to align with each other under thermal fluctuations. Figure 3(a) shows that it is similar to the Fermi-Dirac function. That is, at low temperature the value is close to one but close

to zero at high temperatures. We note that the trailing edges of the curves in the inset of Fig. 3(a) correspond to the first rapid increase of the permittivity in Fig. 2, which shifts to high temperatures with the increase in frequency. Such characteristics are consistent with the fact that polarons are susceptible to thermal fluctuations (and difficult to align with each other), which can easily damage their dielectric response at higher temperatures.

Figure 3(b) shows the permittivity induced by conductivity [the 3rd term in Eq. (5)]. The contribution of conductivity is small below 200 K but increases rapidly beyond this point. This is consistent with the basic assumption of the statistical model that considers thermally activated processes. At higher temperatures, due to the thermal activation, conductive charge carriers start to have a large contribution to the dielectric permittivity. At room temperature, the contribution is about 5 % of the total dielectric permittivity of CCTO, which suggests that, at room temperature, polarons make the most important contribution to the total permittivity.

3.5 Polarons and conductive charge carriers

Zhang *et. al* considered that traces of Ti^{3+} exists in CCTO due to the loss of oxygen from the grains during the high-temperature sintering,²⁸ where the Ti^{3+} and Ti^{4+} can form $\text{Ti}^{3+}\text{-O-Ti}^{4+}$ bonds. The Ti-3d electrons in Ti^{3+} ions can thus hop to Ti^{4+} under an applied electric field. Moreover, the formation of Ti^{3+} ions distorts CCTO lattices since the ionic radius of Ti^{4+} is smaller than that of Ti^{3+} , therefore producing a polaronic distortions. The relaxation time of polarons is larger than that of free electrons because of the polaronic distortion.

In the low-temperature region, polarons stay in more localized states due to the Anderson localization resulting from atom alloying and strain.²⁷ Therefore, E_b of the CCTO could be high, comparable to that of ferroelectric $\text{Ba}(\text{Ti}_{0.9}\text{Zr}_{0.1})\text{O}_3$ and $\text{Ba}(\text{Ti}_{0.8}\text{Zr}_{0.2})\text{O}_3$ discussed in Ref.⁴⁶. In this respect, the dynamic behavior of polarons in CCTO is similar to that of dipoles of normal ferroelectrics. However, the polarization changes in CCTO (due to hoppings of polarons) are conceivably much larger than that of ferroelectrics (due to dipoles on each

lattice site), making the permittivity of CCTO very large. Furthermore, the hopping of charge carriers (polarons) leads to semiconducting grains, which in turn leads to the Maxwell-Wagner effect. The herein proposed model thus helps us to identify the activation energy, and estimate the relative dielectric strength from a different groups of polarons. From this perspective, if we want to increase the polaron contribution, one effective way is to decrease E_b so that more polarons can be excited at room temperature.

It is important to bear in mind that polarons are not the only ones that can make a substantial contribution to the permittivity of CCTO. Since CCTO ceramics consist of semiconducting grains and insulating grain boundaries, the conductivity insides grains increases with temperature (which eventually make a large contribution to the permittivity at high temperatures). Therefore, the Maxwell-Wagner effect, which results in giant dielectric permittivity, starts to be important at the room temperature (see Fig. 1). Further increasing temperature, the diffuse dielectric anomaly is observed, where the electrical conductivity that is associated with thermally activated electrons from Ti-3d electrons in Ti^{3+} ions (the activation energy E_{con} is much lower than that of oxygen vacancies) overcome grain boundaries, becoming high enough to be prominent and need to be included in the permittivity as shown in Eq. 5. While such effects push the permittivity of CCTO to even larger values, the accompanying dielectric loss is so severe that some balance shall be considered to avoid this situation in the design of other dielectric materials similar to CCTO.

4 Conclusions

We have investigated the low frequency 0.5-600 kHz dielectric properties of CCTO over a large temperature range (90 – 500 K). We have proposed an explicit formula to fit the temperature dependence of the dielectric permittivity at different frequencies. Our statistical model can explain well the low temperature step-function-like dielectric relaxation of CCTO and has estimated the activation energy of polarons. The contribution from conductive charge

carriers at high temperatures also plays a key role on the dielectric behavior. We hope that our model and the fitting results will deepen the understanding of the behavior of CCTO resulting from the interplay between the localization and conduction of charge carriers.

Acknowledgement

This work was supported financially by the National Natural Science Foundation of China (NSFC), Grant Nos. 11564010, 11574246, 51390472, and U1537210, and the National Basic Research Program of China, Grant No. 2015CB654903, and the Natural Science Foundation of Guangxi (Grant No. GA139008, CB380006, FA198015).

References

- (1) Subramanian, M. A.; Dong, L.; Duan, N.; Reisner, B. A.; Sleight, A. W. High Dielectric Constant in $ACu_3Ti_4O_{12}$ and $ACu_3Ti_3FeO_{12}$ Phases. *J. Solid State Chem.* **2000**, *151*, 323-325.
- (2) Ramirez, A. P.; Subramanian, M. A.; Gardel, M.; Blumberg, G.; Li, D.; Vogt, T.; Shapiro, S. M. Giant Dielectric Constant Response in a Copper-titanate. *Solid State Commun.* **2000**, *115*, 217-220.
- (3) Homes, C. C.; Vogt, T.; Shapiro, S. M.; Wakimoto, S.; Ramirez, A. P. Optical Response of High-dielectric-constant Perovskite-related Oxide. *Science* **2001**, *293*, 673-676.
- (4) Lin, Y.; Chen, Y. B.; Garret, T.; Liu, S. W.; Chen, C. L.; Chen, L.; Bontchev, R. P.; Jacobson A.; Jiang, J. C.; Meletis, E. I.; Horwitz, J.; Wu, H.-D. Epitaxial Growth of Dielectric $CaCu_3Ti_4O_{12}$ Thin Films on (001) $LaAlO_3$ by Pulsed Laser Deposition. *Appl. Phys. Lett.* **2002**, *81*, 631-633.
- (5) Si, W.; Cruz, E. M.; Johnson, P. D.; Barnes, P. W.; Woodward, P.; Ramirez, A. P.

- Epitaxial Thin Films of The Giant-dielectric-constant Material $\text{CaCu}_3\text{Ti}_4\text{O}_{12}$ Grown by Pulsed-laser Deposition. *Appl. Phys. Lett.* **2002**, *81*, 2056-2058.
- (6) Felix, A. A.; Orlandi, M. O.; Varela, J. A. Schottky-type Grain Boundaries in CCTO Ceramics. *Solid State Commun.* **2011**, *151*, 1377-1381.
- (7) Schmidt, R.; Stennett, M. C.; Hyatt, N. C.; Pokorny, J.; Prado-Gonjal, J.; Li, M.; Sinclair, D. C. Effects of Sintering Temperature on The Internal Barrier Layer Capacitor (IBLC) Structure in $\text{CaCu}_3\text{Ti}_4\text{O}_{12}$ (CCTO) Ceramics. *J. Eur. Ceram. Soc.* **2012**, *32*, 3313-3323.
- (8) Han, F.; Ren, S.; Deng, J.; Yan, T.; Ma, X.; Peng, B.; Liu, L. Dielectric Response Mechanism and Suppressing High-frequency Dielectric Loss in Y_2O_3 Grafted $\text{CaCu}_3\text{Ti}_4\text{O}_{12}$ Ceramics. *J. Mater. Sci.: Mater. Electron.* **2017**, *28*, 17378-17387.
- (9) Deng, J.; Sun, X.; Liu, L.; Liu, S.; Huang, Y.; Fang, L.; Elouadi, B. Dielectric Properties of SrMnO_3 -doped $\text{K}_{0.5}\text{Na}_{0.5}\text{NbO}_3$ Lead-free Ceramics. *J. Adv. Dielect.* **2016**, *6*, No. 1650009.
- (10) Deng, J.; Liu, L.; Sun, X.; Liu, S.; Yan, T.; Fang, L.; Elouadi, B. Dielectric Relaxation Behavior and Mechanism of $\text{Y}_{2/3}\text{Cu}_3\text{Ti}_4\text{O}_{12}$ Ceramic. *Mater. Res. Bull.* **2017**, *88*, 320.
- (11) Neupane, K. P.; Cohn, J. L.; Terashita, H.; Neumeier, J. J. Doping Dependence of Polaron Hopping Energies in $\text{La}_{1-x}\text{Ca}_x\text{MnO}_3$ ($0 \leq x \leq 0.15$). *Phys. Rev. B* **2006**, *74*, No. 144428.
- (12) Freitas, R. S.; Mitchell, J. F.; Schiffer, P. Magnetodielectric Consequences of Phase Separation in The Colossal Magnetoresistance Manganite $\text{Pr}_{0.7}\text{Ca}_{0.3}\text{MnO}_3$. *Phys. Rev. B* **2005**, *72*, No. 144429.
- (13) Wang, C. C.; Cui, Y. M.; Zhang, L. W. Dielectric Properties of TbMnO_3 Ceramics. *Appl. Phys. Lett.* **2007**, *90*, No. 012904.

- (14) Yang, A. M.; Sheng, Y. H.; Farid, M. A.; Zhang, H.; Lin, X. H.; Li, G. B.; Liu L. J.; Liao F. H.; Lin, J. H. Copper Doped EuMnO_3 : Synthesis, Structure and Magnetic Properties. *RSC Adv.* **2016**, *6*, 13928-13933.
- (15) Deng, J.; Yang A.; Farid M. A.; Zhang, H.; Li, J.; Zhang, H.; Li, G.; Liu, L.; Sun, J.; Lin, Synthesis, Structure and Magnetic Properties of $(\text{Eu}_{1-x}\text{Mn}_x)\text{MnO}_{3-\delta}$. *RSC Adv.* **2017**, *7*, 2019-2024.
- (16) Deng, J.; Farid, M. A.; Yang, A.; Zhang, J.; Zhang, H.; Zhang, L.; Qiu, Y.; Yu, M.; Zhu, H.; Zhong, M; Li J.; Li, G.; Liu, L.; Sun, J.; Lin, J. The Origin of Multiple Magnetic and Dielectric Anomalies of Mn-doped DyMnO_3 in Low Temperature Region. *J. Alloys & Compd.* **2017**, *725*, 976-983.
- (17) Li, G.; Chen, Z.; Sun, X.; Liu, L.; Fang, L.; Elouadi, B. Electrical Properties of $\text{AC}_3\text{B}_4\text{O}_{12}$ -type Perovskite Ceramics with Different Cation Vacancies. *Mater. Res. Bull.* **2015**, *65*, 260-265.
- (18) Park, T.; Nussinov, Z.; Hazzard, K. R. A.; Sidorov, V. A.; Balatsky, A. V.; Sarrao, J. L.; Cheong, S.-W.; Hundley, M. F.; Lee, J.-S.; Jia, Q. X.; Thompson, J. D. Novel Dielectric Anomaly in The Hole-Doped $\text{La}_2\text{Cu}_{1-x}\text{Li}_x\text{O}_4$ and $\text{La}_{2-x}\text{Sr}_x\text{NiO}_4$ Insulators: Signature of an Electronic Glassy State. *Phys. Rev. Lett.* **2005**, *94*, No. 017002.
- (19) Rivas, J.; Rivas-Murias, B.; Fondado, A.; Mira, J.; Senaris-Rodriguez, M. A. Dielectric Response of The Charge-ordered Two-dimensional Nickelate $\text{La}_{1.5}\text{Sr}_{0.5}\text{NiO}_4$. *Appl. Phys. Lett.* **2004**, *85*, 6224-6226.
- (20) Wu, J.; Nan, C. W.; Lin, Y.; Deng, Y. Giant Dielectric Permittivity Observed in Li and Ti Doped NiO . *Phys. Rev. Lett.* **2002**, *89*, No. 217601.
- (21) Li, Y.; Fang, L.; Liu, L.; Huang, Y.; Hu, C. Giant Dielectric Response and Charge Compensation of Li-and Co-doped NiO ceramics. *Mater. Sci. Eng. B* **2012**, *177*, 673-677.

- (22) Raevski, I. P.; Prosandeev, S. A.; Bogatin, A. S.; Malitskaya, M. A.; Jastrabik, L. High Dielectric Permittivity in $\text{AFe}_{1/2}\text{B}_{1/2}\text{O}_3$ Nonferroelectric Perovskite Ceramics (A= Ba, Sr, Ca; B= Nb, Ta, Sb). *J. Appl. Phys.* **2003**, *93*, 4130-4136.
- (23) Ke, S.; Lin, P.; Huang, H.; Fan, H.; Zeng, X. Mean-field Approach to Dielectric Relaxation in Giant Dielectric Constant Perovskite Ceramics. *J. Ceram.* **2013**, *2013*, No. 795827.
- (24) Huang, Y.; Shi, D.; Liu, L.; Li, G.; Zheng, S.; Fang, L. High-temperature Impedance Spectroscopy of $\text{BaFe}_{0.5}\text{Nb}_{0.5}\text{O}_3$ Ceramics Doped with $\text{Bi}_{0.5}\text{Na}_{0.5}\text{TiO}_3$. *Appl. Phys. A* **2014**, *114*, 891-896.
- (25) Liu, S.; Sun, X.; Peng, B.; Su, H.; Mei, Z.; Huang, Y.; Deng, J.; Su, C.; Fang, L.; Liu, L. Dielectric Properties and Defect Mechanisms of $(1 - x)\text{Ba}(\text{Fe}_{0.5}\text{Nb}_{0.5})\text{O}_3$ - $x\text{BiYbO}_3$ Ceramics. *J. Electroceram.* **2016**, *37*, 137-144.
- (26) Sun, X.; Deng, J.; Liu, S.; Yan, T.; Peng, B.; Jia, W.; Mei, Z.; Su, H.; Fang, L.; Liu, L. Grain Boundary Defect Compensation in Ti-doped $\text{BaFe}_{0.5}\text{Nb}_{0.5}\text{O}_3$ Ceramics. *Appl. Phys. A* **2016**, *122*, No. 864.
- (27) Wang, C. C.; Zhang, L. W. Polaron Relaxation Related to Localized Charge Carriers in $\text{CaCu}_3\text{Ti}_4\text{O}_{12}$. *Appl. Phys. Lett.* **2007**, *90*, No. 142905.
- (28) Zhang, L.; Tang, Z. J. Polaron relaxation and variable-range-hopping conductivity in the giant-dielectric-constant material $\text{CaCu}_3\text{Ti}_4\text{O}_{12}$. *Phys. Rev. B* **2004**, *70*, No. 174306.
- (29) Tselev, A.; Brooks, C. M.; Anlage, S. M.; Zheng, H.; Salamanca-Riba, L.; Ramesh, R.; Subramanian, M. A. (2004). Evidence for Power-law Frequency Dependence of Intrinsic Dielectric Response in The $\text{CaCu}_3\text{Ti}_4\text{O}_{12}$. *Phys. Rev. B* **2004**, *70*, No. 144101.

- (30) Valdez-Nava, Z.; Guillemet-Fritsch, S.; Tenailleau, C.; Lebey, T.; Durand, B.; Chane-Ching, J. Y. Colossal Dielectric Permittivity of BaTiO₃-based Nanocrystalline Ceramics Sintered by Spark Plasma Sintering. *J. Electroceramics* **2009**, *22*, 238-244.
- (31) Liu, L.; Fan, H.; Wang, L.; Chen, X.; Fang, P. Dc-bias-field-induced Dielectric Relaxation and ac Conduction in CaCu₃Ti₄O₁₂ Ceramics. *Philos. Mag.* **2008**, *88*, 537-545.
- (32) Liu, L.; Shi, D.; Zheng, S.; Huang, Y.; Wu, S.; Li, Y.; Fang, L.; Hu, C. Polaron Relaxation and Non-ohmic Behavior in CaCu₃Ti₄O₁₂ Ceramics with Different Cooling Methods. *Mater. Chem. Phys.* **2013**, *139*, 844-850.
- (33) Bidault, O.; Maglione, M.; Actis, M.; Kchikech, M.; Salce, B. Polaronic Relaxation in Perovskites. *Phys. Rev. B* **1995**, *52*, 4191-4197.
- (34) Mott, N. F.; Davis, E. A. *Electronic Processes in Non-crystalline Solids*. Clarendon: Oxford , 1979.
- (35) Krohns, S.; Lunkenheimer, P.; Ebbinghaus, S. G.; Loidl, A. Colossal Dielectric Constants in Single-crystalline and Ceramic CaCu₃Ti₄O₁₂ Investigated by Broadband Dielectric Spectroscopy. *J. Appl. Phys.* **2008**, *103*, 084107.
- (36) Chung, S. Y.; Kim, I. D.; Kang, S. J. L. Strong Nonlinear Current–Voltage Behaviour in Perovskite-derivative Calcium Copper Titanate. *Nature Mater.* **2004**, *3*, 774-778.
- (37) Kastner, M. A.; Birgeneau, R. J.; Chen, C. Y.; Chiang, Y. M.; Gabbe, D. R.; Jenssen, H. P.; Junk, T.; Peter, C. J.; Picone, P. J.; Thio, T.; Thurston, T. R.; Tuller, H. L. Resistivity of Nonmetallic La_{2-*y*}Sr_{*y*}Cu_{1-*x*}Li_{*x*}O_{4-*δ*} Single Crystals and Ceramics. *Phys. Rev. B* **1988**, *37*, 111-117.
- (38) Ang, C.; Jing, Z.; Yu, Z. Variable-range-hopping Conduction and Metal-insulator Transition in Cu-doped BaTiO₃. *J. Phys.: Condens. Matter* **1999**, *11*, 9703-9708.

- (39) Karmakar, A.; Majumdar, S.; Giri, S. Polaron Relaxation and Hopping Conductivity in $\text{LaMn}_{1-x}\text{Fe}_x\text{O}_3$. *Phys. Rev. B* **2009**, *79*, No. 094406.
- (40) Liu, J.; Li, F.; Zeng, Y.; Jiang, Z.; Liu, L.; Wang, D.; Ye, Z.-G.; Jia, C. L. Insights into The Dielectric Response of Ferroelectric Relaxors from Statistical Modeling. *Phys. Rev. B* **2017**, *96*, No. 054115.
- (41) Raevski, I. P.; Prosandeev, S. A.; Bogatina, A. S.; Malitskaya, M. A., and Jastrabik L. High-k ceramic materials based on nonferroelectric $\text{AFe}_{1/2}\text{B}_{1/2}\text{O}_3$ (A-Ba, Sr, Ca; B-Nb, Ta, Sb) perovskites. *Integrated Ferroelectrics* **2003**, *55*, 757-768.
- (42) Raevski, I. P.; Prosandeev, S. A.; Bogatin, A. S.; Malitskaya, M. A., and Jastrabik L. *J. Appl. Phys.* **2003**, *93*, 4130.
- (43) Maglione M., Free charge localization and effective dielectric permittivity in oxides, *J. Adv. Delect.* 2016, **6**, 163006.
- (44) Kasap, S. O. *Principles of Electronic Materials and Devices*, Third ed; McGraw-Hill: New York, 2006.
- (45) Jonscher, A. K. A New Understanding of The Dielectric Relaxation of Solids. *J. Mater. Sci.* **1981**, *16*, 2037-2060.
- (46) Liu, L.; Ren, S.; Zhang, J.; Peng, B.; Fang, L.; Wang, D. Revisiting The Temperature-dependent Dielectric Permittivity of $\text{Ba}(\text{Ti}_{1-x}\text{Zr}_x)\text{O}_3$. *J. Am. Ceram. Soc.* **2018**, *101*, 2408-2416.